ELECTRONIC SUPPLEMENTARY INFORMATION

Hydrodeoxygenation and hydrodenitrogenation of *n*-hexadecanamide over Pt catalysts: effect of the support

Emma Verkama[a]*, Sylvia Albersberger[b], Aitor Arandia[a†], Kristoffer Meinander[c], Marja Tiitta[b‡], Reetta Karinen[a], Riikka L. Puurunen[a]

[a]Department of Chemical and Metallurgical Engineering, School of Chemical Engineering, Aalto University, P.O. Box 16100, 00076 Aalto, Finland
[b]Neste Corporation, P.O. Box 310, 06101 Porvoo, Finland
[c]Department of Bioproducts and Biosystems, School of Chemical Engineering, Aalto University, P.O. Box 16300, 00076 Aalto, Finland

Present address:
† VTT Technical Research Centre of Finland Ltd. P.O. Box 1000, FI-02044 Espoo, Finland
‡ Haavikkotie 35-37 C 16, FI-06650 Hamari, Finland

* Corresponding author:
Emma Verkama, emma.verkama@aalto.fi

1. Control experiments

The repeatability of the experiments was evaluated by repeating the 60-minute experiment at 300 °C and 80 bar H_2 twice, for the Pt/ZrO_2 catalyst. The 180-minute experiment was also repeated once. A 60-minute activity test was also carried out for a second batch of the Pt/ZrO_2 catalyst to ensure the repeatability of the catalyst preparation. The presence of external diffusion limitations was assessed by carrying out 60-minute activity tests at otherwise identical conditions, but stirring with 200 rpm and 1000 rpm, instead of 600 rpm. The product distribution and nitrogen removal of the experiments are displayed in Figure S1.

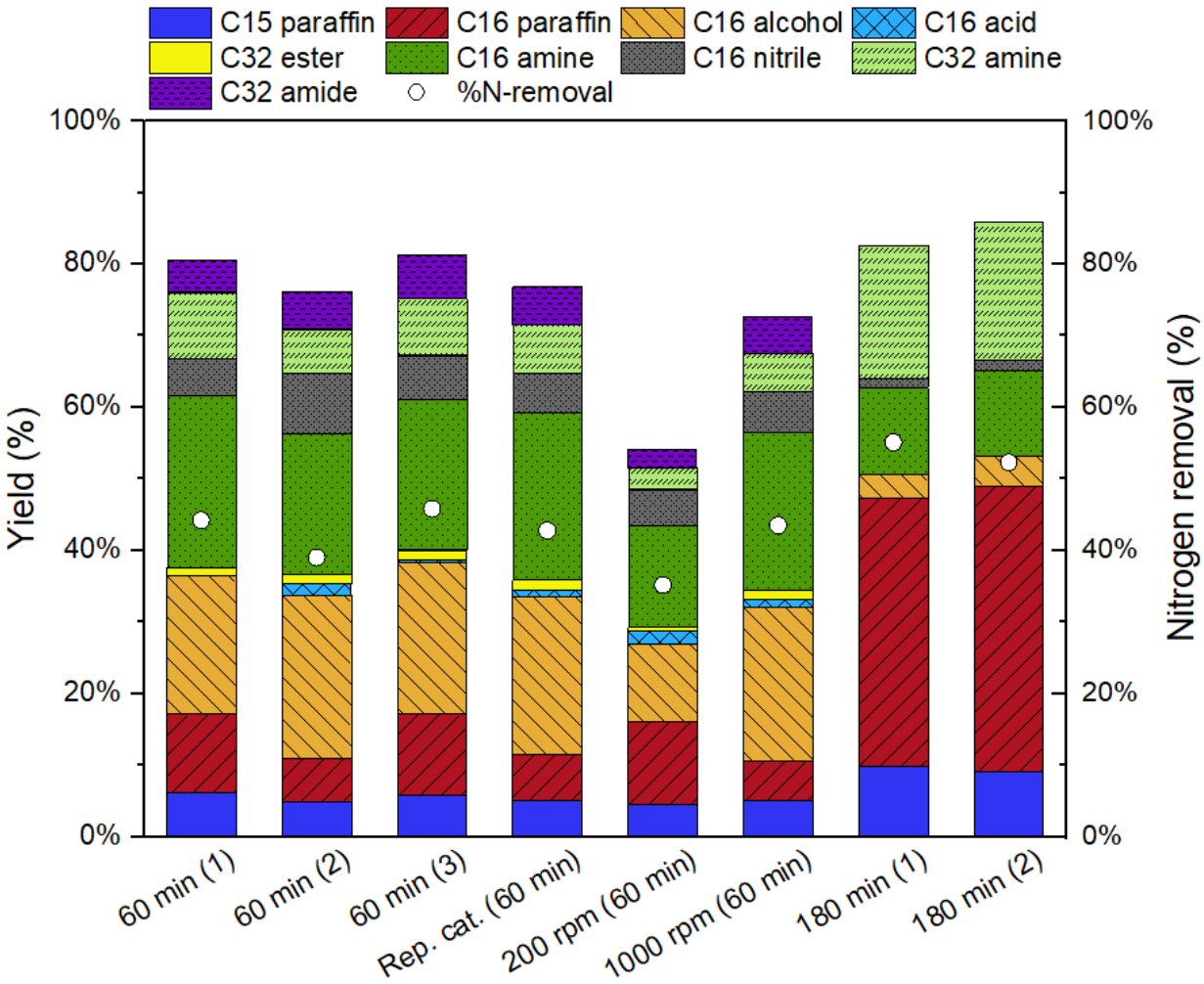

Figure S1. Product distribution and nitrogen removal (○) of the repetition experiments with Pt/ZrO_2, an experiment with a repetition batch of the Pt/ZrO_2 catalyst, and experiments with Pt/ZrO_2 with 200 rpm and 1000 rpm stirring. All experiments were carried out at 300 °C and 80 bar H_2 for 60 or 180 minutes, using 100 ppm N in the feed and 20 mg catalyst.

The product distribution of the three 60-minute experiments carried out with the Pt/ZrO_2 catalysts were similar compared to each other, and to the product distribution of the second batch of Pt/ZrO_2, i.e., the repetition catalyst. The 1st and 3rd experiments were almost identical with each other, whereas

the 2nd experiment appeared to lag slightly behind, as reflected from the nitrogen removal and C16 paraffin yield, both of which were 4-5 percentage points lower compared to the 1st and 3rd experiments. The product distribution of the two 180-minute experiments was similar.

The product distribution, conversion and nitrogen removal of the experiment with 1000 rpm stirring speed was similar to the experiments with 600 rpm stirring speed, indicating that the 600 rpm stirring speed was suitable (Figure S1). A lower conversion and nitrogen removal was obtained for the experiment with 200 rpm, pointing towards external mass transfer limitations. Interestingly, the paraffin yield of the 200 rpm experiment was similar, or even higher, compared to the 600 and 1000 rpm experiments, whereas the yield of C32 compounds was considerably lower.

2. N_2-physisorption isotherms and pore size distribution

Figure S2 displays the N_2-physisorption isotherms of the catalysts. The corresponding Barrett-Joyner-Halenda (BJH) pore size distributions are presented in Figure S3.

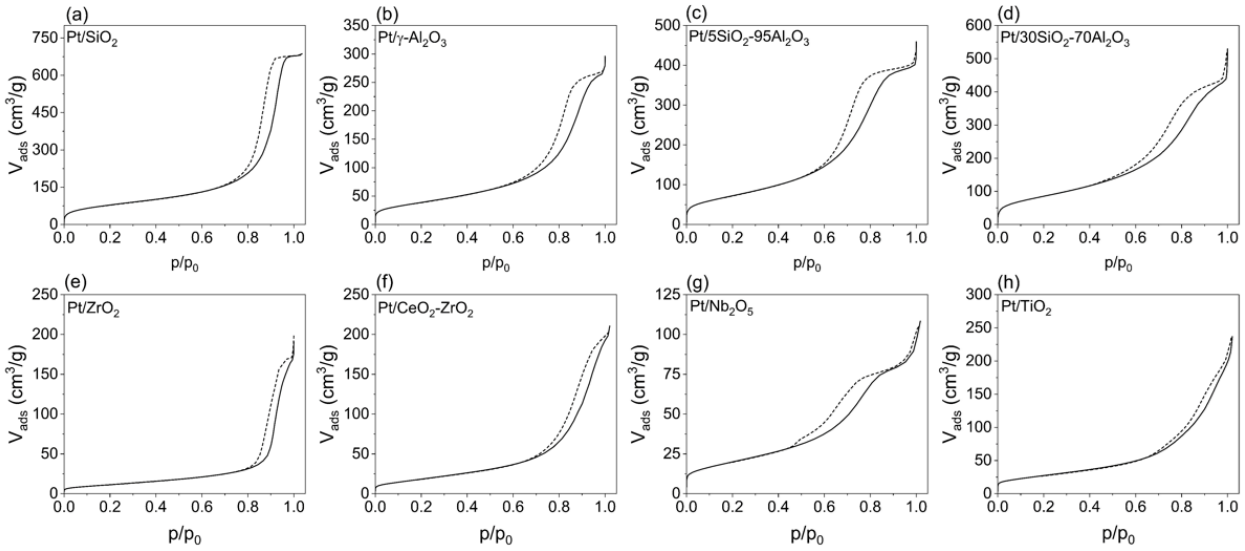

Figure S2. N_2-physisorption isotherms of (a) Pt/SiO_2, (b) $Pt/\gamma\text{-}Al_2O_3$, (c) $Pt/5SiO_2\text{-}95Al_2O_3$, (d) $Pt/30SiO_2\text{-}70Al_2O_3$, (e) Pt/ZrO_2, (f) $Pt/25CeO_2\text{-}75ZrO_2$, (g) Pt/Nb_2O_5 and (h) Pt/TiO_2.

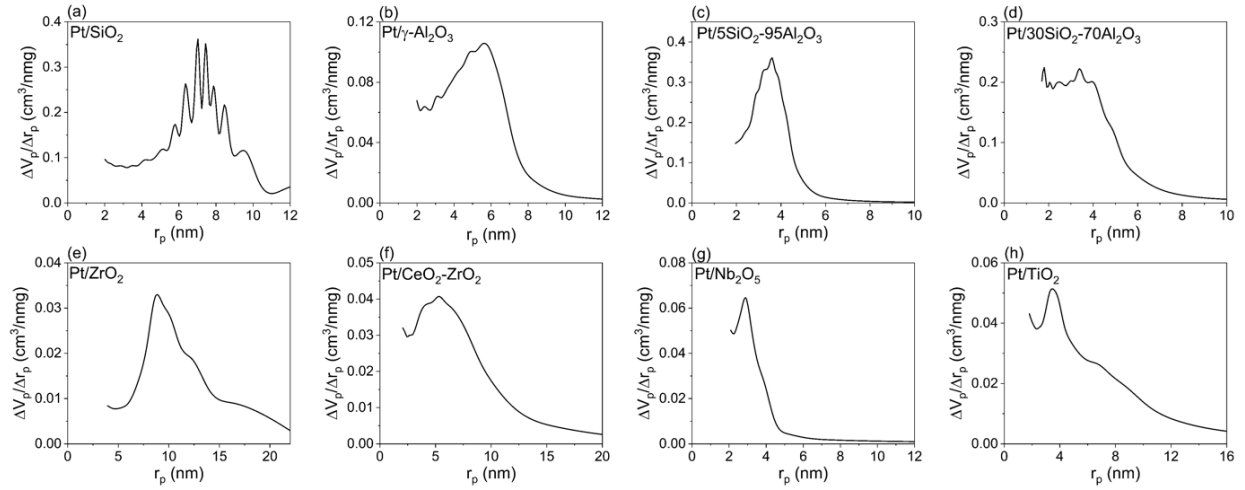

Figure S3. BJH pore size distribution of (a) Pt/SiO_2, (b) $Pt/\gamma\text{-}Al_2O_3$, (c) $Pt/5SiO_2\text{-}95Al_2O_3$, (d) $Pt/30SiO_2\text{-}70Al_2O_3$, (e) Pt/ZrO_2, (f) $Pt/25CeO_2\text{-}75ZrO_2$, (g) Pt/Nb_2O_5 and (h) Pt/TiO_2.

3. Scanning transmission electron microscopy images

Representative examples of scanning transmission electron microscopy (STEM) images of the calcined catalysts are presented in Figure S4. The STEM images of the catalysts displayed regions rich and poor in Pt particles, suggesting that the Pt distribution was heterogeneous. Figure S5 displays the Pt particle size distribution histograms, derived from the STEM images.

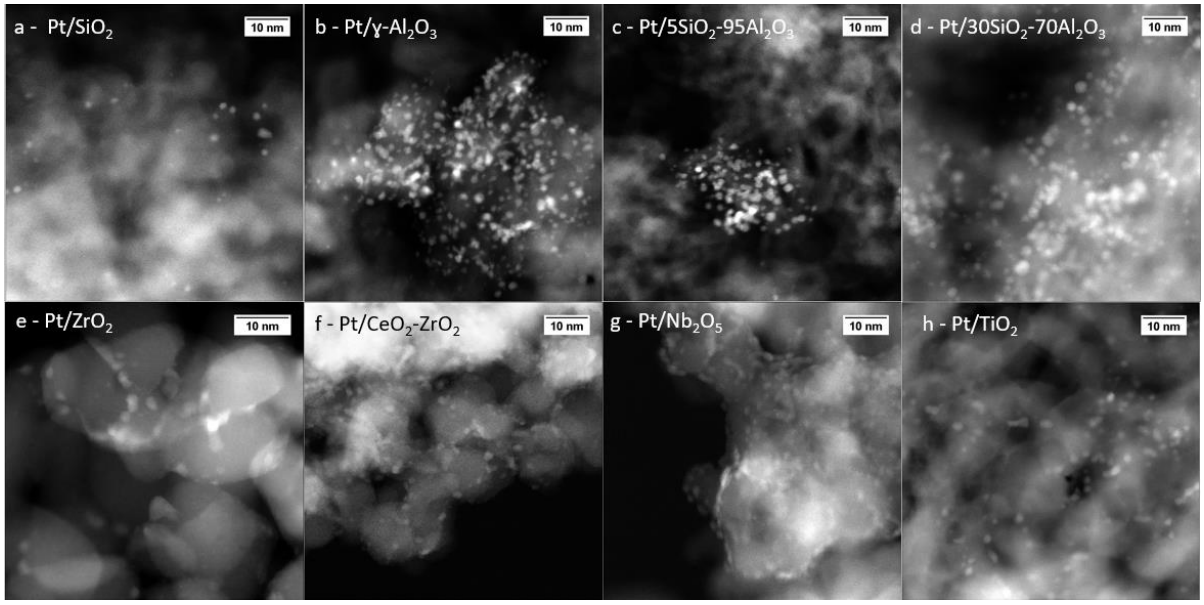

Figure S4. Representative STEM images of (a) Pt/SiO_2, (b) $Pt/ɣ\text{-}Al_2O_3$, (c) $Pt/5SiO_2\text{-}95Al_2O_3$, (d) $Pt/30SiO_2\text{-}70Al_2O_3$, (e) Pt/ZrO_2, (f) $Pt/25CeO_2\text{-}75ZrO_2$, (g) Pt/Nb_2O_5 and (h) Pt/TiO_2.

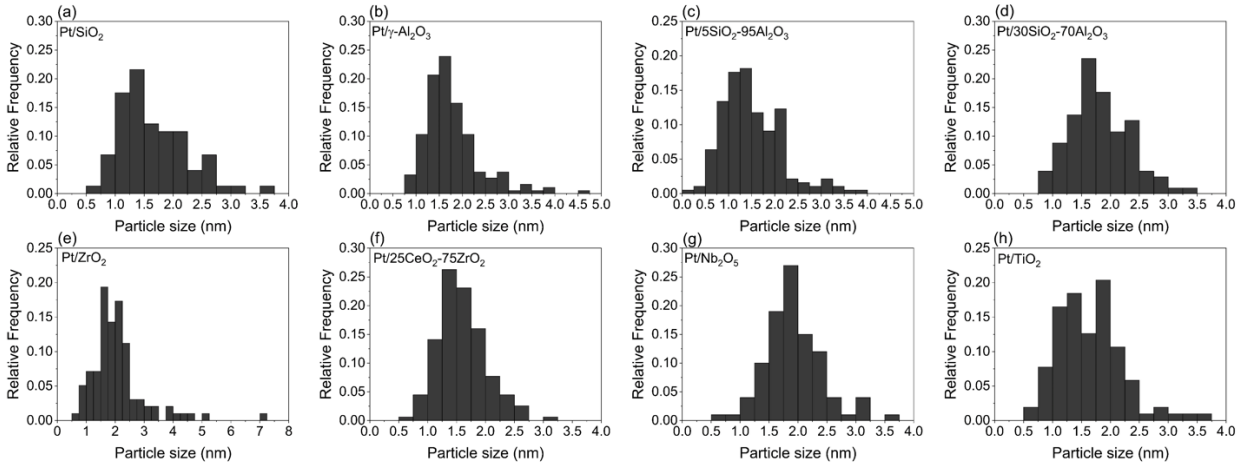

Figure S5. Pt particle size distribution histograms derived from STEM images for (a) Pt/SiO_2, (b) $Pt/ɣ\text{-}Al_2O_3$, (c) $Pt/5SiO_2\text{-}95Al_2O_3$, (d) $Pt/30SiO_2\text{-}70Al_2O_3$, (e) Pt/ZrO_2, (f) $Pt/25CeO_2\text{-}75ZrO_2$, (g) Pt/Nb_2O_5 and (h) Pt/TiO_2.

4. X-ray diffraction

The X-ray diffractograms of the catalysts are displayed in Figure S6. Reflections characteristic to Pt were absent from the X-ray diffractograms of the analyzed catalysts. The X-ray diffractogram of the Pt/SiO_2 catalyst contained one broad reflection at 22°, characteristic for amorphous SiO_2, and the X-ray diffractogram of $Pt/\gamma\text{-}Al_2O_3$ confirmed the desired γ-phase for the support (ICDD 01-075-0921). The X-ray diffractogram of the $Pt/5SiO_2\text{-}95Al_2O_3$ catalyst likewise contained only $\gamma\text{-}Al_2O_3$ related reflections, whereas the X-ray diffractogram of $Pt/30SiO_2\text{-}70Al_2O_3$ (Figure S6d) contained broad reflections characteristic for $\gamma\text{-}Al_2O_3$ at 39.3°, 45.6°, and 66.6°, as well as sharp reflections at 36.9°, 41.2°, 72.5° and 75.5°. The sharp reflections indicate that a partial phase change from $\gamma\text{-}Al_2O_3$, possibly towards $\delta\text{-}Al_2O_3$ (ICDD 00-072-0420, partial match), occurred for Al_2O_3 during calcination of the $30SiO_2\text{-}70Al_2O_3$ support.

A monoclinic phase for the support was confirmed for Pt/ZrO_2 and Pt/Nb_2O_5 (ICDD 00-007-0343 and ICDD 00-027-1312, respectively), whereas the reflections of Pt/TiO_2 corresponded to anatase TiO_2 (ICDD 01-083-5914). The reflections of the X-ray diffractogram $Pt/CeO_2\text{-}ZrO_2$ best matched $Ce_{0.20}Zr_{0.80}O_2$ with a tetragonal phase (ICDD 04-002-5421).

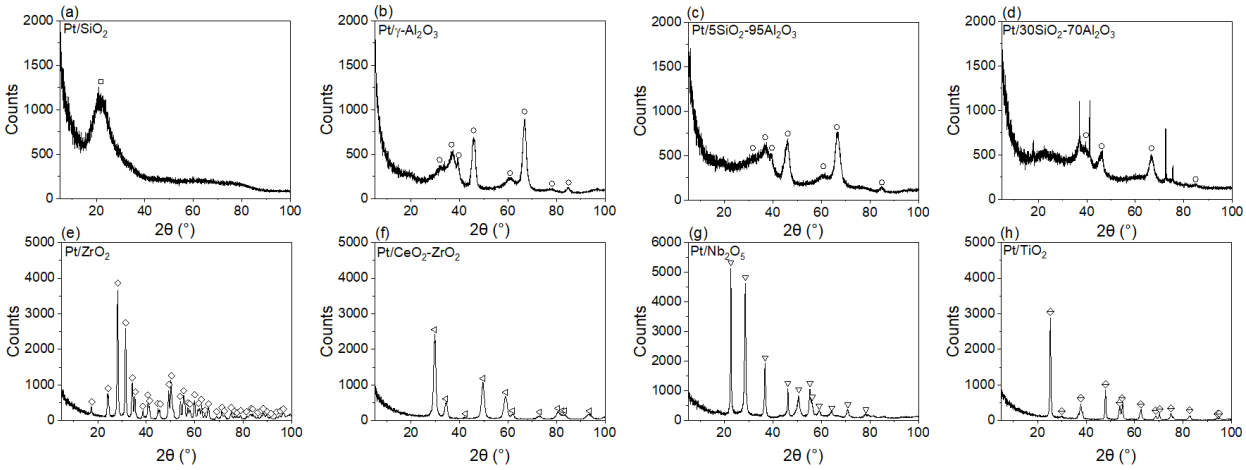

Figure S6. X-ray diffractograms for (a) Pt/SiO_2, (b) $Pt/\gamma\text{-}Al_2O_3$, (c) $Pt/5SiO_2\text{-}95Al_2O_3$, (d) $Pt/30SiO_2\text{-}70Al_2O_3$, (e) Pt/ZrO_2, (f) $Pt/25CeO_2\text{-}75ZrO_2$, (g) Pt/Nb_2O_5 and (h) Pt/TiO_2. The marked reflections correspond to SiO_2 (□), $\gamma\text{-}Al_2O_3$ (○, ICDD 01-075-0921), monoclinic ZrO_2 (◇, ICDD 00-007-0343), tetragonal $Ce_{0.20}Zr_{0.80}O_2$ (◁, ICDD 04-002-5421), monoclinic Nb_2O_5 (▽, ICDD 00-027-1312) and anatase TiO_2 (◈, ICDD 01-083-5914).

5. X-ray photoelectron spectroscopy

The X-ray photoelectron spectroscopy (XPS) survey spectra of the catalysts are displayed in Figure S7.

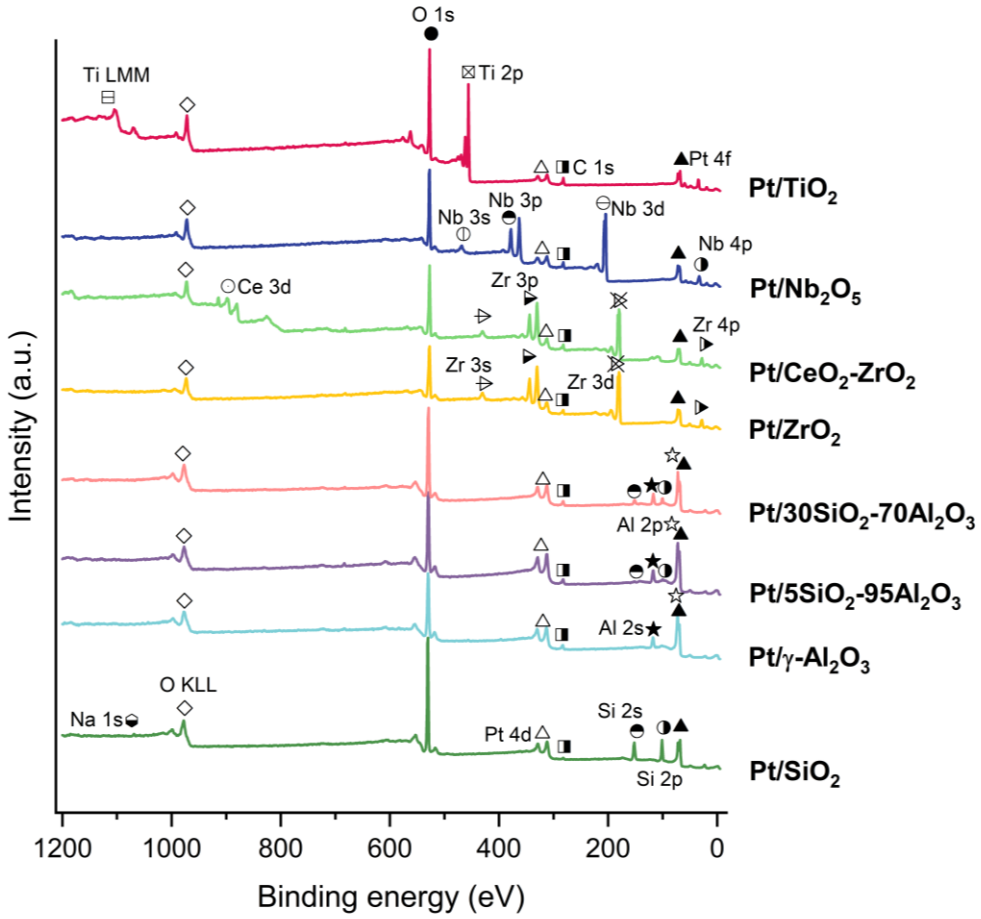

Figure S7. XPS survey spectra of the catalysts.

Table S1 displays the atomic surface composition of the catalysts, obtained from the XPS measurements. Table S2 summarizes the elemental ratio between oxygen and the support cations of the catalysts and the elemental ratio between Pt and the support cations.

Table S1. Atomic surface composition from the XPS measurements

Catalyst	Pt 4f/4d[a] (at. %)	O 1s (at. %)	C 1s (at. %)	Si (at. %)	Al (at. %)	Zr 3d (at. %)	Ce 3d (at. %)	Nb 3d (at. %)	Ti 2p (at. %)	Na (at. %)
Pt/SiO_2	3.4	56.4	2.9	37.0	-	-	-	-	-	0.4
$Pt/\gamma\text{-}Al_2O_3$	5.9	49.4	9.3	-	35.5	-	-	-	-	-
$Pt/5SiO_2\text{-}95Al_2O_3$	6.2	48.5	9.3	2.1	33.9	-	-	-	-	-
$Pt/30SiO_2\text{-}70Al_2O_3$	3.6	49.9	7.3	10.9	28.3	-	-	-	-	-
Pt/ZrO_2	4.9	52.3	12.5	-	-	30.4	-	-	-	-
$Pt/CeO_2\text{-}ZrO_2$	3.9	53.1	14.1	-	-	25.3	3.7	-	-	-
Pt/Nb_2O_5	4.5	55.1	13.8	-	-	-	-	26.7	-	-
Pt/TiO_2	3.2	58.8	12.8	-	-	-	-	-	25.1	-

[a]Pt 4d used for Pt/SiO_2, $Pt/\gamma\text{-}Al_2O_3$, $Pt/5SiO_2\text{-}95Al_2O_3$ and $Pt/30SiO_2\text{-}70Al_2O_3$.

Table S2. Atomic ratio between Pt and the support cations $(Pt/M)_{XPS}$ and atomic ratios between oxygen and the support cations, from the XPS measurements

Catalyst	$(Pt/M)_{XPS}$	O/(1.5Al+2Si)	O/(2Ce+2Zr)	O/2.5Nb	O/2Ti
Pt/SiO_2	0.09	0.76	-	-	-
$Pt/\gamma\text{-}Al_2O_3$	0.17	0.93	-	-	-
$Pt/5SiO_2\text{-}95Al_2O_3$	0.17	0.88	-	-	-
$Pt/30SiO_2\text{-}70Al_2O_3$	0.09	0.78	-	-	-
Pt/ZrO_2	0.16	-	0.86	-	-
$Pt/CeO_2\text{-}ZrO_2$	0.13	-	0.92	-	-
Pt/Nb_2O_5	0.17	-	-	0.82	-
Pt/TiO_2	0.13	-	-	-	1.17

6. Temperature programmed desorption of CO_2

Figure S8 displays the CO_2 desorption profiles of the CO_2-TPD measurements.

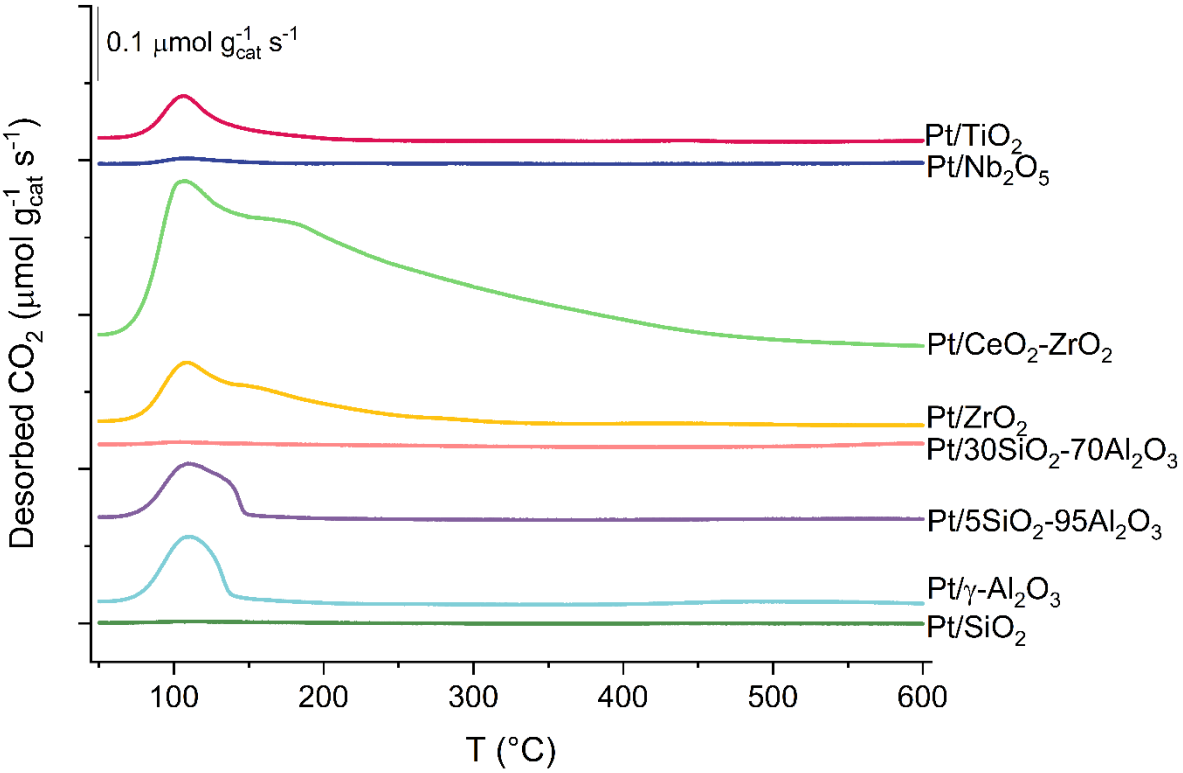

Figure S8. CO_2-TPD profiles of the supported Pt catalysts. The catalysts were reduced at 350 °C for 60 min before the CO_2 saturation at 50 °C.